15th Triennial World Congress, Barcelona, Spain

TWO-DIMENSIONAL CALIBRATION OF A SUN ATTITUDE SENSOR

Roland Strietzel

Jena-Optronik GmbH, an enterprise of Astrium GmbH
Prussingstr. 41, D – 07745 Jena, Germany
Tel.: +49 3641 200 177, Fax: +49 3641 200 220
E-Mail: Roland.Strietzel@jena-optronik.de

Abstract: Attitude sensors are used in spacecrafts for measurement and control of its attitude to meet the mission goals. Sensors using the sun for attitude determination are very effective and often applied. The calibration of the sensor gives an important impetus to improve the quality. Calibration helps to reduce systematic errors of the measurement method, of tolerances of the used components due to manufacturing, deviations in the assembly, misalignment etc. An important advantage of the multi-linear and the spline interpolation is the continuous improvement of the accuracy by increasing the number of calibration coefficients. Both methods are applied to a sun sensor using fuzzy logic. The necessary number of parameters or interpolation cells depends on the global input-to-output behaviour of the sensor and can be predicted by means of a sensor model. Simulations show the ability to compensate systematic errors and allow finding an optimal number of calibration cells. This contribution shows, that effective calibration with the belonging software can reduce the expense of spacecraft hardware. *Copyright © 2002 IFAC*

Keywords: Aerospace engineering, Attitude, Calibration, Error correction, Fuzzy logic, Interpolation, Splines.

1. INTRODUCTION

An important device for attitude measurement and control of spacecrafts is the sun sensor (Ermakov, *et al*., 1997; Wertz, 1997). Sun sensors have a high reliability and are relatively cheep. The accuracy of a Fine Sun Sensors (FSS) is better than 0.1 ° (Schroeter, 1997; Elstner, 1997). Because of the growing interest in the availability of FSS type sensors, here such a sensor is discussed (Strietzel*, et al*., 1998). Aims in designing these sensors were small costs at sufficient accuracy and substitution of hardware by software. In this way a more extensive calibration allows to save expenditure especially in the mechanical hardware. This requires a stabile construction with respect to temperature influence, mechanical stability and electro-magnetic compatibility. The necessary expenditure of calibration depends on the sensor behaviour and the admissible errors. A decisive augmentation of the accuracy one obtains by two-dimensional calibration of the sun sensor.

2. FOUR-QUADRANT SUN SENSOR

The sensor consists of a 4-quadrant photo diode chip, a spacer and a quadratic-dot mask. Depending on the sun incident angles α, β, the light dot illuminates more or less the pixels A, B, C and D. The photo currents of these pixels can be used to calculate the coordinates x, y of the light dot position (Fig. 1).
d is the edge of the quadratic image, x, y describes its location. The isolating distance between the four pixels is s.
Regarding fuzzy logic (Drechsel, 1996), the linguistic input variable u has 4 linguistic values A, B, C and D with their membership functions $\mu(A)$, $\mu(B)$, $\mu(C)$ and $\mu(D)$ representing the belonging photo currents. The values a, d and s are so defined, that between the positions (x, y) within the ranges –

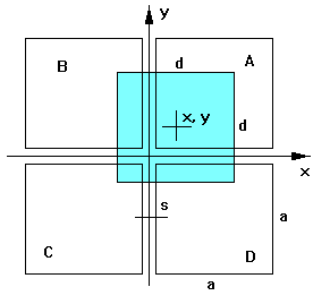

u	v_1	v_2
A	c	c
B	– c	c
C	– c	– c
D	c	– c

Fig. 1. Photodiode array, light dot (a = 3 mm, d = 2.8 mm, s = 0.11 mm) and rule base.

$-x_m \le x \le x_m$ and $-y_m \le y \le y_m$ and the membership functions μ(A), μ(B), μ(C), μ(D) exists a one-to-one transformation. This is necessary to avoid equivocation or information loss in the measurement channel.
The fuzzy unit realises the transformation from the linguistic values to the measured sun angles α_m, β_m (Fig. 2). With the calibration algorithm these angles are corrected to α_c, β_c.

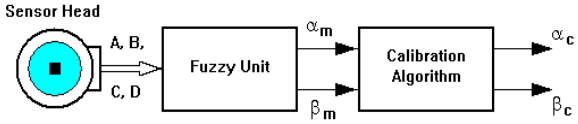

Fig. 2. Signal flow diagram.

The 4 linguistic values (A, B, C, D) contain all the information about the values x and y in Fig. 1.
Fig. 1 gives also the rule base of the inference for the linguistic outputs v_1 and v_2. The values of the inference outputs v_1 and v_2 are – c and c with the membership values μ(– c) and μ(c).
As inference method the so-called Sum-Prod inference is used. On this base one obtains following membership values of the inference outputs:
output v_1:

$$\mu_1(c) = \mu(A) + \mu(D),\ \mu_1(-c) = \mu(B) + \mu(C), \quad (1)$$

output v_2:

$$\mu_2(c) = \mu(A) + \mu(B),\ \mu_2(-c) = \mu(C) + \mu(D). \quad (2)$$

The defuzzification operation of the both linguistic output fuzzy sets v_1 and v_2 yields the dot coordinates x and y using the centre of gravity method for singletons,

$$x = c\,[\mu(A) - \mu(B) - \mu(C) + \mu(D)] / S, \quad (3)$$

$$y = c\,[\mu(A) + \mu(B) - \mu(C) - \mu(D)] / S, \quad (4)$$

$$S = \mu(A)+\mu(B)+\mu(C)+\mu(D). \quad (5)$$

The amount c determines the amplification between input and output. Under the condition of the avoidance of information loss and a symmetric arrangement according to Fig. 1 one obtains:

$$x_m = (d - s)/2,\ a \ge d - s, \quad (6)$$

$$y_m = (d - s)/2. \quad (7)$$

The membership functions μ(A), μ(B), μ(C), μ(D) can be replaced by corresponding photo currents i_A, i_B, i_C, i_D.
To verify the algorithm of Equ. (3), (4) and (5), the photo currents i_A, i_B, i_C, i_D of the arrangement in Fig. 1 are calculated,

$$i_A = I_o\,(d/2 + x - s/2)\,(d/2 + y - s/2), \quad (8)$$
$$i_B = I_o\,(d/2 - x - s/2)\,(d/2 + y - s/2), \quad (9)$$
$$i_C = I_o\,(d/2 - x - s/2)\,(d/2 - y - s/2), \quad (10)$$
$$i_D = I_o\,(d/2 + x - s/2)\,(d/2 - y - s/2). \quad (11)$$

The currents depend on the current efficacy I_o of the photo diodes and the illuminated part of the pixel surface.
The output signals x_{out}, y_{out} result by combining the Equ. (3) to (11),

$$x_{out} = 2\,c\,x\,/(d - s),\ \ y_{out} = 2\,c\,y\,/(d - s) \quad (12)$$

With $c = (d - s)/2$ one gets $x_{out} = x$, $y_{out} = y$ and

$$x_{out} = (d - s)/2\,[i_A - i_B - i_C + i_D]/[i_A + i_B + i_C + i_D], \quad (13)$$

$$y_{out} = (d - s)/2\,[i_A - i_B - i_C + i_D]/[i_A + i_B + i_C + i_D]. \quad (14)$$

This simple structure allows the measurement of sun incident angles α_m, β_m, if the quadratic image is produced by a suitable mask and a spacer determining a definite distance h between mask and chip. The equations

$$\alpha_m = \arctan(x_{out}/h),\ \beta_m = \arctan(y_{out}/h), \quad (15)$$

give the necessary relations.
The results demonstrate, that the measurements α_m and β_m are independent of each other.

3. TECHNICAL REALISATION OF THE SENSOR

The following example describes a technical realisation of a sun sensor according to the above-mentioned principle.

Table 1. Sources of systematic errors

Phase	Example	Deviation	Error
Design	Reflection, diffraction	not considered	
Manu-facturing	Spacer tolerance	± 0.02 mm	± 1 °
	Sensitivity of photo diodes	± 2 %	± 2 °
Assembly	Displacement of the chip	± 0.02 mm	– 2 °
	Rotation	0.2 °	± 0.4 °
	Inclination of the chip	0.2 °	± 0.2°
Operation	Temperature	no	no

This example considers a set of possible disturbances of the sensor behaviour caused by design, manufacturing, assembly and operation.
The regarded effects are listed in Table 1. The influences are composed to a worst-case behaviour. The simulation results of the systematic errors dalpha and dbeta of both sun angles α, β are computed with MATLAB and presented in Fig. 3 and 4.
The relatively small deviations and tolerances given in Table 1 cause errors, which forbid the application of the non-calibrated sensor.

4. NECESSITY OF SENSOR CALIBRATION

Generally the following inaccuracies can disturb the sensor behaviour:

- systematic errors of the measurement method (e.g. nonlinearities)
- deviation of the origin of the mask
- tolerances of the image size
- rotation between mask and sensor chip
- dark currents of the pixels
- different pixel sensitivity (the sensitivity does not depend on the pixel surface) etc.

The calibration and correction procedure consists of the following steps:

- measurement of the sun angles α, β at all the interpolation nodes and determination of the errors of α and β
- calculation of the interpolation coefficients for the concerning interpolation cell
- calculation the correcting values for the measured sun sensor outputs and correction.

The influences of above-mentioned inaccuracies can be decisively reduced by sensor calibration, if these errors are stable. Generally the mentioned disturbances cause interactions between both sun angles. In this case of the two-dimensional calibration the corrected sun incident angles α_c, β_c are functions of the measured sun angles α_m, β_m and two-dimensional error correcting functions,

$$\alpha_c = \alpha_m + \varepsilon_\alpha(\alpha_m,\beta_m),\ \beta_c = \beta_m + \varepsilon_\beta(\alpha_m,\beta_m). \qquad (16)$$

The aim of calibration is the determination of the correcting functions $\varepsilon_\alpha(\alpha,\beta)$ and $\varepsilon_\beta(\alpha,\beta)$ by means of series of discrete measurements in the operational range of the sensor. During calibration the values $\varepsilon_\alpha(\alpha_i,\beta_j) = \varepsilon_\alpha(i,j)$, $\varepsilon_\beta(\alpha_i,\beta_j) = \varepsilon_\beta(i,j)$, i = 0, 1, ... m, j = 0, 1, ... n, at the node i,j are measured as differences

$$\varepsilon_\alpha(\alpha_i,\beta_j) = \alpha_i - \alpha_m(\alpha_i,\beta_j),\ \beta = \beta_j, \qquad (17)$$

$$\varepsilon_\beta(\alpha_i,\beta_j) = \beta_j - \beta_m(\alpha_i,\beta_j),\ \alpha = \alpha_i. \qquad (18)$$

α_i and β_j are the adjusted sun angles at the sun sensor test bench. $\alpha_m(\alpha_i,\beta_j)$ and $\beta_m(\alpha_i,\beta_j)$ are the measured values of the sun incident angles by the sensor under the conditions α_i and β_j without correction. N = (m+1)(n+1) calibration points are used.

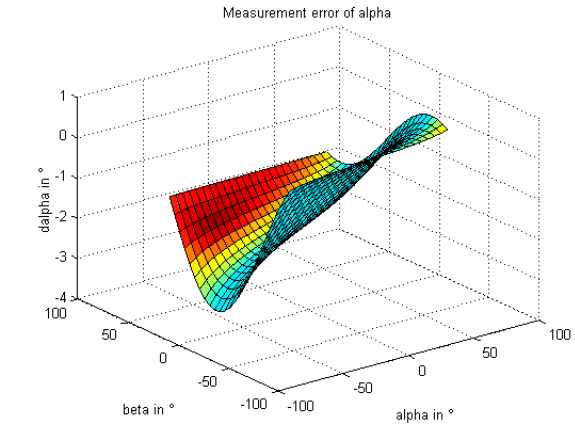

Fig. 3. Measurement error dalpha of the sun angle α depending on the angles α and β.

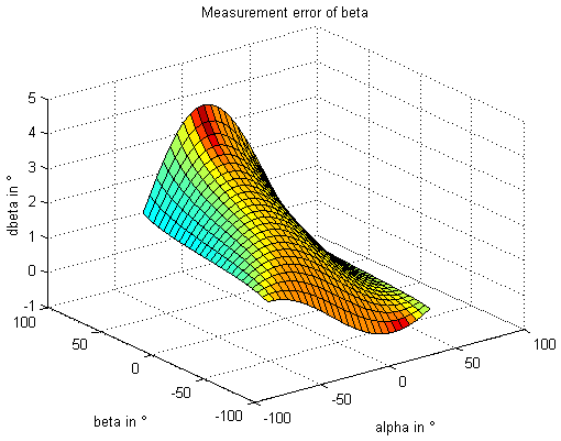

Fig. 4. Measurement error dbeta of the sun angle β depending on the angles α and β.

To obtain continuous correction functions $\varepsilon_\alpha(\alpha,\beta)$ and $\varepsilon_\beta(\alpha,\beta)$ from the discrete measurements according to Equs. (17) and (18), a two-dimensional interpolation algorithms must be applied. So these functions are calculated by means of the errors $\varepsilon_\alpha(\alpha_i,\beta_j)$ and $\varepsilon_\beta(\alpha_i,\beta_j)$ at the predefined interpolation nodes.
For the correction according to Equ. (16) real-time computation is required.
Between the Equ. (16) and the Equs. (17) and (18) exists a principal difference. The error correcting functions $\varepsilon_\alpha(\alpha_m,\beta_m)$ and $\varepsilon_\beta(\alpha_m,\beta_m)$ refer to the inexact measured values and $\varepsilon_\alpha(\alpha_i,\beta_j)$ and $\varepsilon_\beta(\alpha_i,\beta_j)$ to the exact values of the nodes. In the case of sufficiently small errors ε_α and ε_β, the difference can be neglected and $\varepsilon_\alpha(\alpha_m,\beta_m)$, $\varepsilon_\beta(\alpha_m,\beta_m)$ can be obtained by interpolation on the base of $\varepsilon_\alpha(\alpha_i,\beta_j)$ and $\varepsilon_\beta(\alpha_i,\beta_j)$.
If the amounts of errors are relatively high in relation to the interpolation step, then the following procedure should be applied:
With the Equs. (16) the corrected values α_{mc} and β_{mc} are calculated,

$$\alpha_{mc} = \alpha_m + \varepsilon_\alpha(\alpha_m,\beta_m),\ \ \beta_{mc} = \beta_m + \varepsilon_\beta(\alpha_m,\beta_m). \quad (19)$$

α_{mc} and β_{mc} are used to calculate a better approach of the correcting functions ε_α, ε_β. So one obtains

$$\alpha_c = \alpha_m + \varepsilon_\alpha(\alpha_{mc},\beta_{mc}),\ \beta_c = \beta_m + \varepsilon_\beta(\alpha_{mc},\beta_{mc}) \quad (20)$$

for the corrected sensor outputs.
This method is used in the case of Fig. 3 and Fig. 4.
The specification of the interpolation depends on the following aspects:

- the number of interpolation nodes
- the order of the interpolation polynomial
- the number of characterising parameters
- the computational expenditure for the error correction.

Global interpolation methods like Lagrange and Newton Interpolation are not used here. Therefore for the example of the proposed sun sensor a comparison of the multi-linear and the cubic spline interpolation is performed.

5. MULTI-LINEAR INTERPOLATION

The elementary interpolation cell is sketched in Fig. 5 (Drechsel, 1996). The step sizes amount

$$h_1 = \alpha_{i+1} - \alpha_i, \qquad h_2 = \beta_{j+1} - \beta_j \quad (21)$$

for equidistant interpolation nodes. If m is the number of intervals in α-direction and n in β-direction, then one has $M = m{\cdot}n$ interpolation cells and $N = (m+1)(n+1)$ interpolation nodes. Each node requires one measurement for one angle. Because of the symmetry of the operational ranges, $m = n$ is defined.
α_i, β_j are the sun angle values at the nodes i or j respectively. $\varepsilon(\alpha_i,\beta_j) = \varepsilon(i,j)$ is the error at the interpolation node i, j according to Equs. (16).

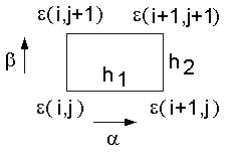

Fig. 5. Elementary interpolation cell

The assumed linear edge functions in α-direction

$$\varepsilon_{11} = \varepsilon(\alpha_i,\beta_j)\,(\alpha_{i+1} - \alpha)/h_1 + \varepsilon(\alpha_{i+1},\beta_j)\,(\alpha - \alpha_i)/h_1, \quad (22)$$
$$\varepsilon_{12} = \varepsilon(\alpha_i,\beta_{j+1})\,(\alpha_{i+1} - \alpha)/h_1 + \varepsilon(\alpha_{i+1},\beta_{j+1})\,(\alpha - \alpha_i)/h_1, \quad (23)$$

allow the interpolation over the whole surface of the cell within the interpolation nodes $\varepsilon(\alpha_i,\beta_j)$, $\varepsilon(\alpha_{i+1},\beta_j)$, $\varepsilon(\alpha_i,\beta_{j+1})$, $\varepsilon(\alpha_{i+1},\beta_{j+1})$ by combining the results of the edge interpolations ε_{11}, ε_{12}. One obtains

$$\varepsilon(\alpha,\beta) = \varepsilon_{11}\,(\beta_{i+1} - \beta)/h_2 + \varepsilon_{12}\,(\beta - \beta_i)/h_2, \quad (24)$$

The interpolation can be performed also in β-direction. Both variants lead to the same result:

$$\begin{aligned}\varepsilon(\alpha,\beta) = {} & \varepsilon(\alpha_i,\beta_j)\,(\alpha_{i+1} - \alpha)/h_1\,(\beta_{j+1} - \beta)/h_2 + \\ & + \varepsilon(\alpha_{i+1},\beta_j)\,(\alpha - \alpha_i)/h_1\,(\beta_{j+1} - \beta)/h_2 + \\ & + \varepsilon(\alpha_i,\beta_{j+1})\,(\alpha_{i+1} - \alpha)/h_1\,(\beta - \beta_j)/h_2 + \\ & + \varepsilon(\alpha_{i+1},\beta_{j+1})\,(\alpha - \alpha_i)/h_1\,(\beta - \beta_j)/h_2 \end{aligned} \quad (25)$$

With the abbreviations

$$\Delta\alpha = \alpha - \alpha_i,\ \Delta\beta = \beta - \beta_j \quad (26)$$

the following polynomial arises

$$\varepsilon(\alpha,\beta) = g_\beta'\, A\, g_\alpha. \quad (27)$$
$$g_\alpha = (1\ \Delta\alpha)',\ g_\beta = (1\ \Delta\beta)', \quad (28)$$

with

$$A = \begin{pmatrix} a_{oo} & a_{o1} \\ a_{1o} & a_{11} \end{pmatrix}, \quad (29)$$

$$a_{oo} = \varepsilon(\alpha_i,\beta_i), \quad (30)$$
$$a_{o1} = [\varepsilon(\alpha_{i+1},\beta_i) - \varepsilon(\alpha_i,\beta_i)]/h_1, \quad (31)$$
$$a_{1o} = [\varepsilon(\alpha_i,\beta_{i+1}) - \varepsilon(\alpha_i,\beta_i)]/h_2, \quad (32)$$
$$a_{11} = [\varepsilon(\alpha_i,\beta_i) - \varepsilon(\alpha_{i+1},\beta_i) - \varepsilon(\alpha_i,\beta_{i+1}) + \varepsilon(\alpha_{i+1},\beta_{i+1})]/(h_1 h_2). \quad (33)$$

This bilinear interpolation requires for one elementary cell only four coefficients, which are easy to calculate.
The result of calibration is summarised in a list of N coefficients characterising the individual sun sensor.

6. SPLINE INTERPOLATION

Unlike to the multi-linear interpolation, the spine interpolation generates smooth interpolation functions (Engeln-Müllges and Reutter, 1996). For the calibration of an attitude sensor for measuring two sun incident angles the following cubic spline interpolation specification seems to be useful:

- two-dimensional interpolation (error depends on the sensitive and insensitive sun angle)
- equidistant interpolation nodes (behaviour of the error function)
- marginal partial derivatives are not available
- vanishing marginal second derivatives (natural splines)
- cubic spline (reduction of the number of interpolation nodes)
- no fitting splines (noise level is smaller than systematic errors).

Each cell has its own interpolation function $f_{ij}(x,y)$. This interpolation polynomial has the form

$$f_{ij}(x,y) = g_x(x)'\, A\, g_y(y) \quad (34)$$

$$g_x(x) = [g_{i0}(x)\ g_{i1}(x)\ g_{i2}(x)\ g_{i3}(x)]'$$
$$g_y(y) = [g_{j0}(y)\ g_{j1}(y)\ g_{j2}(y)\ g_{j3}(y)]' \quad (35)$$

with the vector elements

$$g_{i0}(x) = 1,\ g_{i1}(x) = x - x_i\ ,\ g_{i2}(x) = (x - x_i)^2,$$
$$g_{i3}(x) = (x - x_i)^3, \quad (36)$$
$$g_{i0}(y) = 1,\ g_{j1}(y) = y - y_j\ ,\ g_{j2}(y) = (y - y_j)^2,$$
$$g_{j3}(y) = (y - y_j)^3, \quad (37)$$

and the coefficient matrix

$$A_{ij} = \begin{bmatrix} a_{ij00} & a_{ij01} & a_{ij02} & a_{ij03} \\ a_{ij10} & a_{ij11} & a_{ij12} & a_{ij13} \\ a_{ij20} & a_{ij21} & a_{ij22} & a_{ij23} \\ a_{ij30} & a_{ij31} & a_{ij32} & a_{ij33} \end{bmatrix}. \quad (38)$$

For the example of the sun sensor, the variable x refers to the angle α and y to β. Each interpolation cell i, j needs 16 coefficients. The character of the coefficient results from Equ. (34). After the cell description i, j the third index of the elements of the matrix A_{ij} describes the power of the belonging variable $x - x_i$ and the fourth the power of the of the variable $y - y_j$.
The calculation of the coefficient matrix requires a series of operations on the base of the values $f(x_i, y_j)$ at the interpolation nodes to determine the partial derivatives $\partial/\partial x\ f(x_i, y_j) = a_{ij10}$, $\partial/\partial y\ f(x_i, y_j) = a_{ij01}$, $\partial^2/(\partial x \partial y)\ f(x_i, y_j) = a_{ij11}$:

- calculation of the partial derivatives of the marginal region
- calculation of the interpolation matrices for the x- and y-direction
- calculation of coefficient matrix for the current cell.

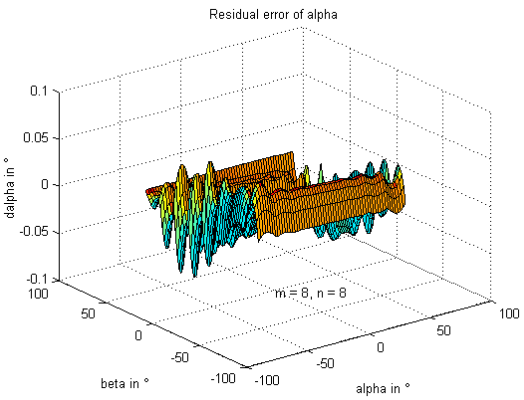

Fig. 6. Residual error of α at multi-linear interpolation (m = n = 8), maximum error ± 0.08 °.

The calculations can be simplified for equidistant and equal steps over the operational range
The result of calibration is the number of N values $f(x_i, y_j)$ at the interpolation nodes. This set characterises the individual sensor. To realise the data transmission for the correction according to the Equ. (16) during the mission, there are diverse possibilities from the N values $f(x_i, y_j)$ at the interpolation nodes up to 16 M cell coefficients for computing Equ. (38) for each cell, depending on the computational abilities onboard.
The calculations show, that the spline interpolation requires more computational expense than the multi-linear interpolation.
By means of the example of a sun sensor the properties of both interpolation methods for calibration shall be compared in the following chapter.

7. COMPARISON OF THE CALIBRATION METHODS

The comparison of the calibration methods on the base of multi-linear and spline interpolation is performed for the sensor characteristics according to section 3. Figures 3 and 4 show, that the uncalibrated sensor has measurement errors of the sun angles of about 4 ° in an operational range of $-60\ ° \le \alpha, \beta \le 60\ °$. This error can be reduced decisively by calibration.
The Figures 6 to 8 show the results of error correction with multi-linear and spline interpolation respectively. They demonstrate the residual error after correction.

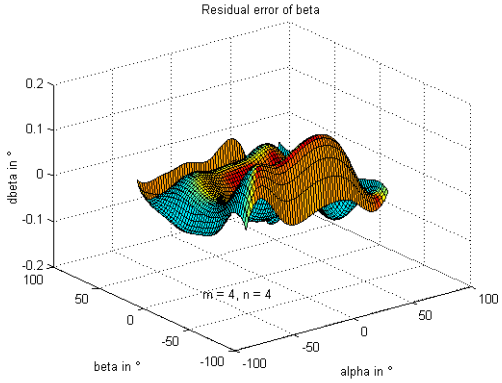

Fig. 7. Residual error of β at spline interpolation (m = n = 4), maximum error ± 0.15 °.

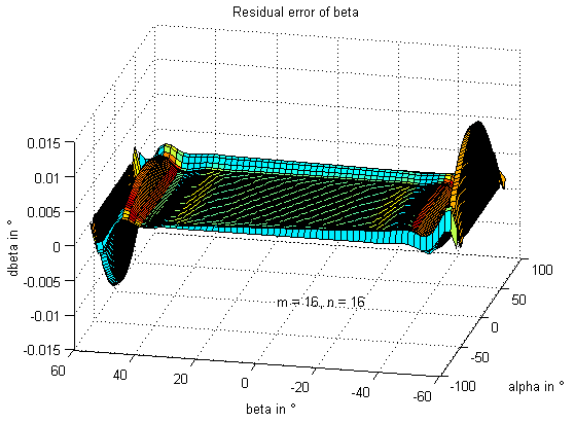

Fig. 8. Example of residual error at spline interpolation with m = n = 16.

The Figures 6 to 8 show, that for approximately the same errors the multi-linear interpolation needs a

higher number of interpolation cells than the spline interpolation. The spline interpolation gives smooth error functions, but the necessary computational expenditure is relatively high.
Fig. 8 demonstrates that at high numbers of interpolation cells the residual errors can be reduced to very small values, excluding the marginal regions. These regions require a special treatment.
The simulation results for different numbers of interpolation intervals are summarised in Table 2.

Table 2. Comparison between linear and spline interpolation

m	N	4 M, 16 M	error /° (pp)	RMS error /°	F_1	F_2
1	start		5	1.18		
Linear interpolation						
8	81	256	0.16	0.031	30	38
16	289	1024	0.04	0.0076	120	155
32	1089	4096	0.01	0.0019	480	621
Spline interpolation						
4	25	256	0.30	0.064	16	18
8	81	1024	0.10	0.014	50	84
16	289	4096	0.02	0.0026	250	453

pp is peak-to-peak.

The maximum error values in Table 2 are peak-to-peak values. The practically interesting maximum error is the half of the written value. The reduction factors F_1 and F_2 describe the relation between the maximum errors and the RMS errors before and after the calibration, respectively. Referring to the third column containing the total number of coefficients for both cases, the comparison in Table 2 shows, that spline interpolation is not so effective than linear interpolation. The disadvantages of linear interpolation are the missing smoothness and the high number of calibration nodes. Spline needs a smaller number of nodes. The software expenditure required by spline interpolation is relatively high.

8. CONCLUSIONS

The calibration of the sensor gives an important impetus to improve the quality of a measuring device. Calibration helps to reduce systematic errors of the measurement method, of tolerances of the used components due to manufacturing, tolerances and deviations in the assembly of components, misalignment etc. Depending on the sensor behaviour and the applicable expenditure some different calibration methods are used. An important advantage of the multi-linear and the spline interpolation is the continuous improvement of the accuracy by increasing the number of interpolation nodes and the avoidance of marginal oscillations.
A successful exchange of hardware expenditure for error correcting software requires a stabile hardware construction with respect to temperature influence, mechanical stability and electro-magnetic compatibility. In this way it is possible, to increase the accuracy of a fuzzy sun sensor decisively.
Linear and spline interpolation are useful methods for sensor calibration. Higher accuracy at a given number of interpolation nodes can be obtained by spline interpolation. But this method requires relatively high software expenditure. Therefore it is recommended to try first with linear interpolation. If the results are not sufficient at a useful number of interpolation nodes and if a high smoothness of the output signal is required, then spline interpolation should be applied. Simulation of the error behaviour of the calibrated sensor supports this decision.
The number of interpolation nodes depends on the structure (especially the smoothness) of the measurement error as function of the both sun angles and determines the measurement expenditure during calibration.
This contribution shows that effective calibration with the belonging software can reduce the expense of hardware, especially with respect to manufacturing and assembly. The example of the fuzzy sun sensor shows, how a relatively simple device can reach a sufficient accuracy.

The author wishes to thank the colleagues of the Jena-Optronik GmbH, especially Ms. Karin Schroeter, for the support and the helpful discussions.

REFERENCES

Drechsel, D. (1996). *Regelbasierte Interpolation und Fuzzy Control.* Vieweg, Braunschweig, Wiesbaden (Deutschland).

Elstner, Ch. (1997). Precision Sun Sensor PSS. International Conference on Space Optics, Toulouse (France).

Engeln-Müllges, G. and F. Reutter (1996). *Numerik-Algorithmen.* VDI Verlag, Duesseldorf.

Ermakov, O. I., I.V. Soloviov and Y.A. Strelchonok (1997). A New Generation of the Sun and Earth Sensors. International Workshop on Spacecraft Attitude and Orbit Control Systems. Noordwijk (The Netherlands).

Schroeter, K. (1997). Development and Application of a Fine Sun Sensor. International Conference on Space Optics, Toulouse (France).

Strietzel, R., W. Skarus and D. Ratzsch (1998). Lagesensorik – Einsatzbereiche, Loesungen, Entwicklungstendenzen. Deutscher Luft- und Raumfahrtkongress 1998, Bremen (Deutschland), *Jahrbuch,* **Band II**, S. 1095 – 1103.

Wertz, J. R. (1997). *Spacecraft Attitude Determination and Control.* Kluwer Academic Publishers, Dordrecht, Boston, London.